Variable resolution imaging fiber probe using digital spatial light modulator

Shinde, Anant; Perinchery, Sandeep Menon; Matham, Murukeshan Vadakke

2015

Shinde, A., Perinchery, S. M., & Matham, M. V. (2015). Variable resolution imaging fiber probe using digital spatial light modulator. Proceedings of SPIE - International Conference on Optical and Photonic Engineering (icOPEN2015), 9524, 95242F-. doi:10.1117/12.2189669

https://hdl.handle.net/10356/89533

https://doi.org/10.1117/12.2189669

Variable resolution imaging fiber probe using digital spatial light modulator

Anant Shinde[ab], Sandeep Menon Perinchery[ab], Murukeshan Vadakke Matham*[ab]
[a]Centre for Optical and Laser Engineering, 50 Nanyang Avenue, Singapore 637798; [b]School of Mechanical and Aerospace Engineering, Nanyang Technological University, Singapore

ABSTRACT

Flexible fiber optic imaging systems including fiber optic confocal probes have found tremendous significance in the recent past for its applications in high resolution imaging. However, motorized stage is required for scanning the sample or tip of the fiber in fiber based confocal probes. In this context, we propose a fiber probe confocal system using digital spatial light modulator devoid of using a mechanical scanning stage. Each fiberlet in the image fiber acts not only as a light conduit but also as a confocal pinhole. The paper also introduces the variation in the contrast by varying the number of illuminated fiberlets which effectively implies variation in the effective pinhole size. This approach has enabled the probe to act as an imaging unit with resolution that can be controlled and varied from a wide-field to a confocal.

Keywords: Fiber optic imaging bundle, confocal fiber imaging, pixelation, variable pinhole, DMD, quasi confocal

1. INTRODUCTION

Diagnostic and therapeutic endoscopic procedures for internal organs of the human body have become quite common in the recent past. Endoscopes are mainly of three types namely tip chip videoscope, rod lens endoscope and flexible fiberscope. Visual access for rod lens endoscopes are restricted by their rigid structure[1]. For tip chip videoscope, size is limited by external light source used to illuminate the sample[2]. Small size and flexibility facilitate fiberscope for visual inspection of narrow and complex passages of medical intra cavities, such as colon and Gastro-Intestinal (GI) tract[3-6]. Fiber Optic Imaging Bundle (FOIB) is the conduit for image transfer in fiberscopes. FOIB is widely used to improve the resolution of endoscopic systems[4, 7-9]. Additionally, FOIB is also utilized in Fiber Optic Confocal Scanning Microscopes[2, 4, 10-15].

However, most of the work in FOIB imaging is confined to either widefield imaging or focused on achieving confocality[9, 10, 16-22]. Confocal imaging involves scanning of very small laser beam over enface of FOIB proximal end adopting several reported scanning methods such as galvanometric mirror scanning, focusing lens scanning, rotating polygon mirror scanning, and rotating Nipkow disc[7, 18, 23]. There are few limitations with these techniques. The beam size in these methods cannot be changed with ease as the pinhole size is controlled by mechanical components. Further, the beam reaching the FOIB enface may not be collimated completely into the core of the fiberlet during scanning. This paper in this context, proposes and demonstrates the use of a digital spatial light modulator, known as Digital Micromirror Device (DMD), for selective illumination of fiberlets at the proximal enface of the FOIB. The paper also demonstrates the precise control of light collimation into the fiberlets core via DMD. This proposed fiber probe imaging system can effectively control the contrast as well as the resolution by selectively varying the effective pinhole size using DMD.

2. IMPACT OF PINHOLE ON FOIB IMAGING

FOIB is a collection of thousands of single mode fibers known as fiberlets[2, 9]. A single mode fiberlet usually has a diameter of 2-4μm. Arrangement of the fiberlets in FOIB remains unchanged over the length of the FOIB. This coherent arrangement allows FOIB to transfer image from one end to the other end of fiber in an efficient manner. Each of these fiberlets act as a light conduit, which creates perfect excitation pinhole[19]. This facilitates, coupling of the illumination light into a single fiberlet at the proximal end to guide it through and emanate from

*mmurukeshan@ntu.edu.sg; phone 65 6790 4200; ntu.edu.sg/home/mmurukeshan/

International Conference on Optical and Photonic Engineering (icOPEN 2015), edited by Anand K. Asundi, Yu Fu,
Proc. of SPIE Vol. 9524, 95242F · © 2015 SPIE · CCC code: 0277-786X/15/$18 · doi: 10.1117/12.2189669

the distal end. Appropriate lens system at the distal end of the FOIB and correct placement of the sample allows collection of reflected light by the same fiberlet through which the sample is illuminated. In FOIB imaging, effective numbers of fiberlets define the effective pinhole size, which has role similar to that of a pinhole in conventional Confocal Laser Scanning Microscopes(CLSM)[3].

There are three different imaging modalities associated to FOIB imaging based on the pinhole size. They are namely wide field, quasi confocal and confocal imaging. FOIB is used mainly as a wide field reflection imaging modality [19, 20]. In wide field reflection configuration, each fiberlet picks signals from the point in front of the fiberlet and also from the points located away from the fiberlet. Figure 1 shows the concept of wide field image formation of FOIB, where light emitted from points $p(x, y + \Delta y)$ to $p(x, y - \Delta y)$ is coupled into the fiberlet to form an image point p'(x, y). Extending the analogy to two dimensional sample and image plane, it can be inferred that in a wide field imaging method, an image point p'(x, y) from an image plane not only depends on the sample point $p(x, y)$ but also on all other sample points that falls in the radius of $r = \sqrt{\Delta x^2 + \Delta y^2}$ from point $p(x, y)$in the sample plane. Here, Δx and Δy represent slight variation from initial position of x and y respectively.

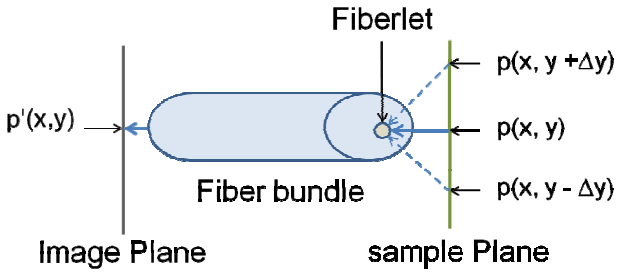

Figure 1. Image formation in wide field imaging

Genrally, wide-field FOIB imaging method, since the complete sample is illuminated and the reflected intensity from the target surface's field of view is collected through the FOIB, results in poor image contrast. In the case of quasi confocal FOIB imaging, more than one fiberlet or a group of fiberlets are used for excitation and collection. Image quality in quasi confocal is better than widefield. In confocal FOIB imaging, a fiberlet from fiber bundle (shown in Figure 1) illuminate the sample point $p(x, y)$ and collect fluorescence light from the same point and transfer it to the other end of fiber so as to be detected by photo detector to form an image point p'(x, y) in an image plane. This result in greater image contrast compared to quasi and wide field methods.

However, FOIB has certain limitations when pinhole diameter is considered, the smallest achievable pinhole diameter for FOIB is size of the core of a single fiberlet (2-4 μm). Full confocality using the FOIB imaging can be achieved when illumination and collection is effected through a smallest pinhole size, which is a single fiberlet. This also suggests that the smallest increment in the pinhole diameter represent addition of one or more fiberlets to the effective pinhole. Pinhole diameter is mainly dictated by the packing fraction and core to core distance of FOIB.

3. MATERIALS AND METHODS

In order to demonstrate the proposed methodology, test samples of thin fluorescent films were prepared using glass bubble, fluorescent dye and polyvinyl alcohol (PVA) in pure water. Initially, PVA is dissolved in warm water followed by mixing it with glass bubbles (30μm) and Rhodamine 6G. Finally, the prepared mixture is transferred onto a glass slide surface and allowed it to solidify and form thin films. The thickness of the film and concentration of the fluorescent dye were optimized to achieve reasonable signal strength during imaging.

Figure 2 shows the schematic of FOIB optical imaging setup. A 30mW, 532nm diode pumped solid state laser is used as the illumination light source. The laser beam is further expanded by a beam expander (BE06R, Thorlabs). Expanded laser beam is impinged on and reflected from DMD (0.7 XGA DDR DMD, Texas Instruments) with selected spatial patterns towards dichroic mirror. Dichroic mirror then reflects this spatially controlled laser light through microscope objective to collimate into thin FOIB of 1.2mm diameter (Sumitomo Electric, Japan). FOIB has 50,000 individual fiberlets, each fiberlet has an average core diameter of 2.7μm and

the average center to center distance between two neighboring fiberlets is 4.4µm. Appropriate optical filter is selected to block the light reflected from the proximal end of FOIB and to allow fluorescence from sample towards the camera. Fluorescence signal from the sample is collected by EMCCD camera (Andor iXon 887).

In this proposed probe embodiment, effective implementation of variable pinhole diameter is realized by properly configuring the optics as well as by implementing the DMD at the desired angle with the optic axis. DMD is able to precisely control the illuminations of the FOIB proximal enface by selectively switching the micromirrors. Additionally, a custom GRIN lens is designed for the FOIB to focus the light and collect emission from the same point of the sample.

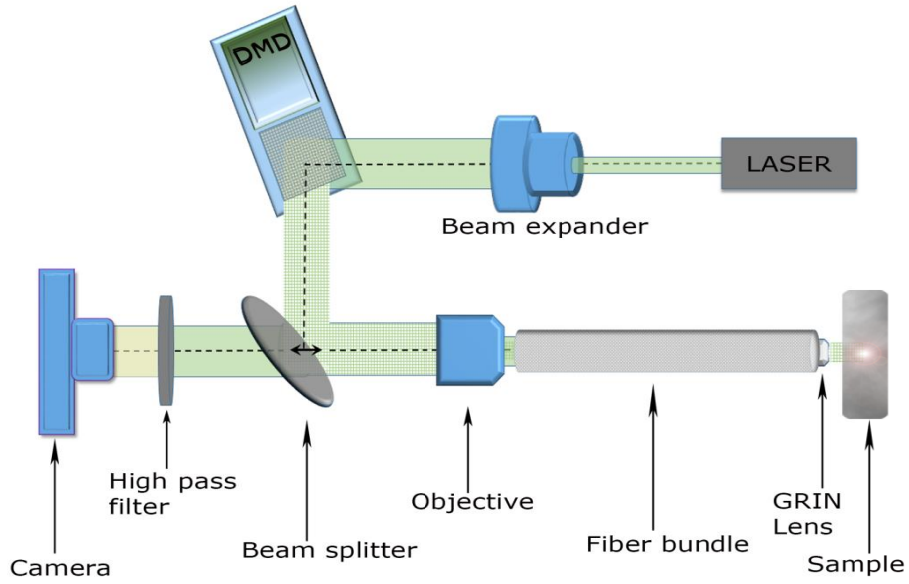

Figure 2. Schematic diagram for the multi-modality optical setup.

4. RESULTS

Capability of the imaging setup using DMD to precisely illuminate desired number of fiberlets of FOIB has been demonstrated. As presented in Figure 3, various illumination patterns were coupled into the FOIB with the optical setup. Further in Figure 4, selection and illumination of single fiberlet (2.7µm) is demonstrated, it shows the full potential of DMD based optical setup. By selective illumination of a single fiberlet using DMD, allowed the FOIB imaging system to have confocality.

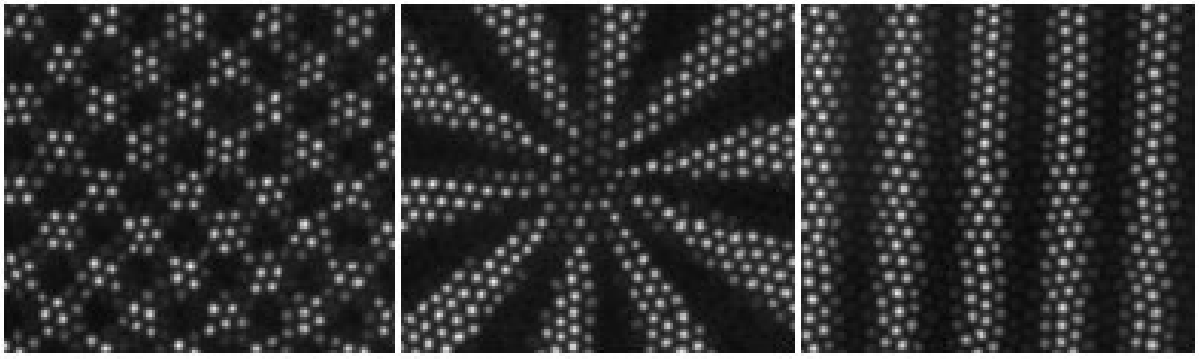

Figure 3. Selective illumination of fiberlets using DMD

Further the effect of variation of pinhole size on the image contrast area was investigated. Figure 4 shows images of a glass bubble collected with imaging modalities having four different pinhole sizes (2.7µm, 7.1µm,

16μm and ROI size). These varying pinhole sizes classify imaging resolution that can be achievable by fully confocal, quasi confocal and wide-field imaging. It is evident from Figure 4 that improved contrast is observed with smaller pinhole size. With increase in pinhole diameter the intensity difference of the pixels showing bright region and dark region reduces. Intensity difference of bright and dark region reduces with increase in pinhole diameter and remains constant for d > 20μm, d is effective pinhole diameter. It also signify that in optical setup described, imaging system is not confocal or quasi-confocal but it is wide-field imaging system for d > 20μm.

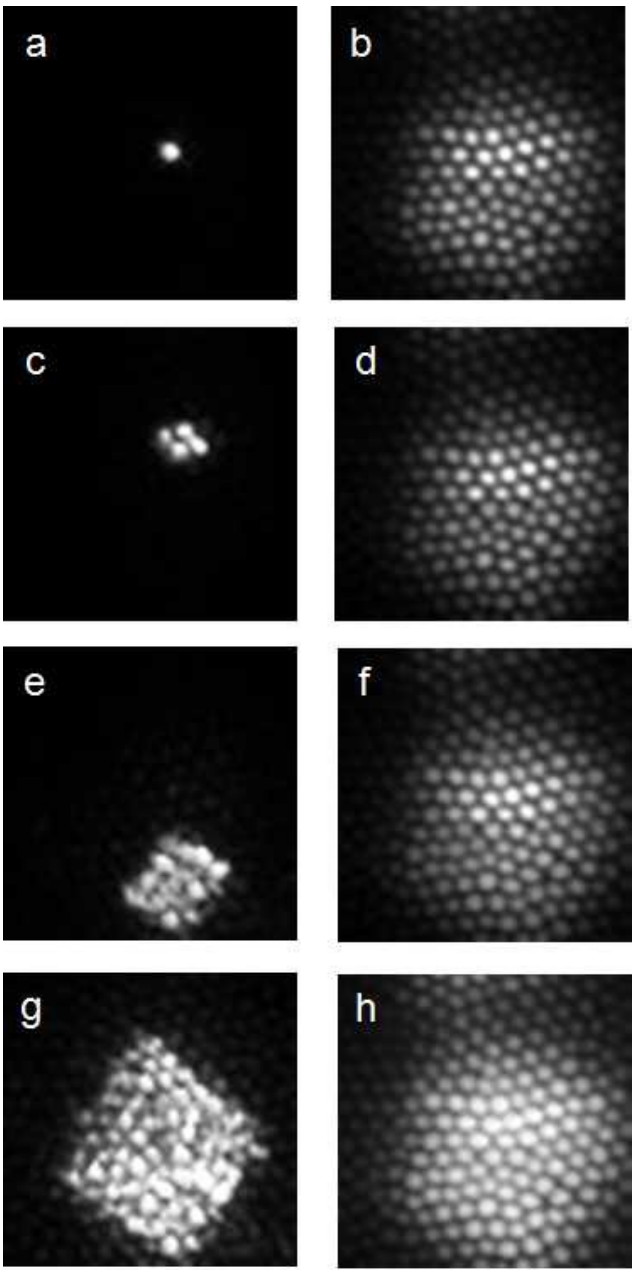

Figure 4. Illustration of glass bubble images with different pinhole sizes. Image a, c and e show proximal end image of FOIB illuminated through pinhole diameter size of one fiberlet, two fiberlet and four fiberlet respectively. Images b, d and f show the entire reconstructed glass bubble images corresponding to different pinhole sizes, one fiberlet, two fiberlet and four fiberlet respectively. Images g and h show the wide-field illumination and image reconstruction of glass bubble.

Further, quantitative evaluation of contrast value for imaging modalities with four different pinhole sizes was performed. To calculate contrast, two different regions of the image were selected. First region was chosen inside the region of glass bubble (non-fluorescing) I_{glass} and second region was outside the bubble (fluorescing area) I_{fluoro}. Contrast value is calculated as,

$$C = \frac{I_{glass} - I_{fluoro}}{I_{glass} + I_{fluoro}}$$

Calculated contrast values and respective pinhole diameter are listed in Table 1. The results show that the image contrast decreases with increase in the pinhole size, validating contrast dependency on pinhole diameter.

Table 1. Contrast variation against pinhole diameter

Pinhole diameter	Contrast
2.7μm,	0.312
7.1μm	0.284
16μm	0.259
Wide-field	0.055

Further, the combination of DMD with FOIB was used for investigation into axial sectioning. To quantify the sectioning ability, sample was moved in Z direction in steps of 2μm and confocal images were captured at every location[21]. Figure 5 shows the Half Width Half Maximum (HWHM) of intensity for full fiber confocal imaging. As evident from the graph, axial resolution of the system (FWHM) is ~4.5um.

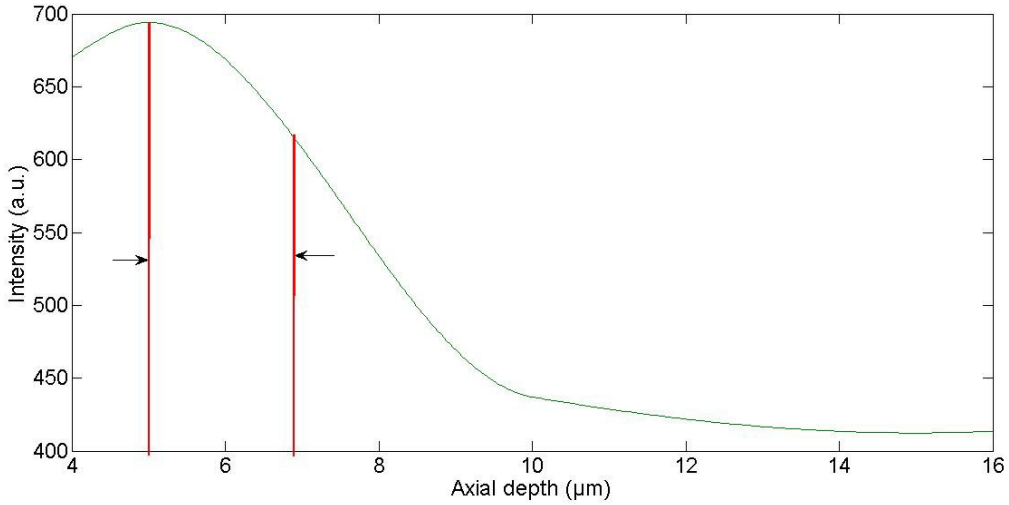

Figure 5. HWHM for full fiber confocal imaging modality

5. CONCLUSION

High resolution FOIB imaging system using DMD has been developed. The potential of the developed probe imaging system to collimate precise patterns of light beam in to FOIB is demonstrated. Additionally, single fiberlet illumination feature is shown. This paper also presented variable contrast imaging by selectively controlling the number of fiberlets illuminated. Further, using DMD for single fiberlet illumination, fiber confocality with axial sectioning is demonstrated.

REFERENCES

[1] Ozawa, T., Tsuchida, M., Yamazaki, Y., and Arai, T., "Minimally invasive periapical curettage of foreign materials in periapical lesions using a fiberscope," International Dental Journal, 53(5), 314-322 (2003).

[2] Murukeshan, V. M., Sujatha, N., Ong, L. S., and Seah, L. K., "Imaging considerations in a fiber optic system for the gastrointestinal endoscopy." Proc. SPIE 5143, 170-180 (2003).

[3] Sathiyamoorthy, K., Mohankumar, V. K., and Murukeshan, V. M., "Real Time Monitoring of Fluorescent Particles in Micro-Channels by High Resolution Dual Modality Probe Imaging," Optics and Photonics Journal, 1(4), 197-203 (2011).

[4] Sujatha, N., Murukeshan, V. M., Ong, L. S., and Seah, L. K., "An all fiber optic system modeling for the gastrointestinal endoscopy: Design concepts and fluorescent analysis," Optics Communications, 219(1-6), 71-79 (2003).

[5] Lee, C. M., Engelbrecht, C. J., Soper, T. D., Helmchen, F., and Seibel, E. J., "Scanning fiber endoscopy with highly flexible, 1 mm catheterscopes for wide-field, full-color imaging," Journal of biophotonics, 3(5-6), 385-407 (2010).

[6] Sandeep, P. M., Rajeev, S. W. B., Sheeba, M., Bhat, S. G., and Nampoori, V. P. N., "Laser induced fluorescence based optical fiber probe for analyzing bacteria," Laser physics letters, 4(8), 611-615 (2007).

[7] Shin, H.-J., Pierce, M. C., Lee, D., Ra, H., Solgaard, O., and Richards-Kortum, R., "Fiber-optic confocal microscope using a MEMS scanner and miniature objective lens," Opt. Express, 15(15), 9113-9122 (2007).

[8] Watanabe, H., Hayashi, J.-i., Takahashi, M., Takekubo, M., and Tosaka, Y., "Aortic Root Endoscopy in Pediatric Cardiac Operations for Aortic Valvuloplasty," Journal of Cardiac Surgery, 17(5), 398-399 (2001).

[9] Murukeshan, V. M., Sujatha, N., Seah, L. K., and Ong, L. S., "All fiber optic endoscope probe distal end for disease diagnosis in body cavities." Proc. SPIE 5651, 321-328.

[10] Benschop, J., and Van Rosmalen, G., "Confocal compact scanning optical microscope based on compact disc technology," Appl. Opt., 30(10), 1179-1184 (1991).

[11] Kimura, S., and Wilson, T., "Confocal scanning optical microscope using single-mode fiber for signal detection," Appl. Opt., 30(16), 2143-2150 (1991).

[12] Kung-Bin, S., Chen, L., Descour, M., Collier, T., Follen, M., and Richards-Kortum, R., "Fiber-optic confocal reflectance microscope with miniature objective for in vivo imaging of human tissues," IEEE Transactions on Biomedical Engineering, 49(10), 1168-1172 (2002).

[13] Gu, M., Sheppard, C. J. R., and Gan, X., "Image formation in a fiber-optical confocal scanning microscope," J. Opt. Soc. Am. A, 8(11), 1755-1761 (1991).

[14] Carlson, K., Chidley, M., Sung, K.-B., Descour, M., Gillenwater, A., Follen, M., and Richards-Kortum, R., "In vivo fiber-optic confocal reflectance microscope with an injection-molded plastic miniature objective lens," Appl. Opt., 44(10), 1792-1797 (2005).

[15] Gu, M., and Sheppard, C. J. R., "Three-dimensional optical transfer function in a fiber-optical confocal fluorescence microscope using annular lenses," J. Opt. Soc. Am. A, 9(11), 1991-1999 (1992).

[16] Winter, C., Rupp, S., Elter, M., Munzenmayer, C., Gerhauser, H., and Wittenberg, T., "Automatic Adaptive Enhancement for Images Obtained With Fiberscopic Endoscopes," IEEE Transactions on Biomedical Engineering, 53(10), 2035-2046 (2006).

[17] Suter, M., Reinhardt, J., Montague, P., Taft, P., Lee, J., and Zabner, J., "Bronchoscopic imaging of pulmonary mucosal vasculature responses to inflammatory mediators," Journal of Biomedical Optics, 10(3), 034013-034013 (2005).

[18] Flusberg, B. A., Cocker, E. D., Piyawattanametha, W., Jung, J. C., Cheung, E. L., and Schnitzer, M. J., "Fiber-optic fluorescence imaging," Nature methods, 2(12), 941-950 (2005).

[19] Mohankumar, V. K., Padmanabhan, P., Murukeshan, V. M., Joseph, J., Sathiyamoorthy, K., and Bhakoo, K. K., "High resolution optical imaging of epithelial and neuronal cells," Journal of Medical Imaging and Health Informatics, 1(4), 354-359 (2011).

[20] Mohankumar, V. K., Sathiyamoorthy, K., and Murukeshan, V. M., “Measurement and contouring of micro-scale objects through integrated transillumination in a flexible fiber probe system,” Optical Engineering, 51(7), 073602-1-073602-5 (2012).
[21] Shinde, A., and Murukeshan, V. M., "Synthetically generated fiber pixilated image database." Proc. SPIE 9128, 91280K-1- 91280K-11 (2014).
[22] Shinde, A., and Matham, M. V., “Pixelate removal in an image fiber probe endoscope incorporating comb structure removal methods,” Journal of Medical Imaging and Health Informatics, 4(2), 203-211 (2014).
[23] Meleppat, R. K., Matham, M. V., and Seah, L. K., “An efficient phase analysis-based wavenumber linearization scheme for swept source optical coherence tomography systems,” Laser Physics Letters, 12(5), 055601 (2015).